International Journal of Mass Spectrometry 295 (2010) 78–84

Contents lists available at ScienceDirect

International Journal of Mass Spectrometry

journal homepage: www.elsevier.com/locate/ijms

Electron impact ionization cross-sections of *n*-heptane

J.R. Vacher[a,b,*], F. Jorand[a,b], N. Blin-Simiand[a,b], S. Pasquiers[a,b]

[a] Univ Paris-Sud, Laboratoire de Physique des Gaz et des Plasmas, UMR 8578, Orsay F-91405, France
[b] CNRS, Orsay F-91405, France

ARTICLE INFO

Article history:
Received 9 June 2010
Received in revised form 8 July 2010
Accepted 9 July 2010
Available online 15 July 2010

Keywords:
Mass spectrometry
Ionization cross-section
VOCs decomposition
n-Heptane

ABSTRACT

Electron impact ionization of *n*-heptane was studied using mass spectrometry. Cross-sections for the formation of molecular ion and ionic fragments are measured between 10 eV and 86 eV with a total cross-section of 1.5×10^{-16} cm^2 towards 50 eV. The molecular ion is the most abundant below 16 eV. The present results display good agreement between the measured total ionization cross-sections and the calculated one with the BEB model. Five ions $C_nH_{2n+1}^+$ ($2 \le n \le 6$) result from a simple C–C bond split in the molecular ion. $C_3H_7^+$, identified as isopropyl cation, is the most abundant of the ionic species above 16 eV. Four ions $C_nH_{2n}^+$ ($2 \le n \le 5$) result from a C–C bond split with H-atom rearrangement. $C_3H_6^+$, identified as propene cation, is the most abundant of these four cations above 35 eV. Five other ions, $C_nH_{2n-1}^+$ ($2 \le n \le 4$), cyclopropenyl and methyl cations may result from the ionization of C_4H_9, the major alkyl issued from the fragmentation of the molecular ion.

1. Introduction

Combustion of fossil fuels is still today a major source of energy in the world. Heptane is a component of commercial gasoline and one of the primary reference fuels for the determination of the gasoline octane number. Progress in minimizing environmental pollution associated with hydrocarbon combustion requires the continuing development of kinetic models. Consequently, the combustion research community has endeavoured to develop detailed chemical kinetic mechanisms for the combustion of heptane. The oxidation of *n*-heptane was experimentally investigated in different systems and modelling studies were undertaken [1–5]. Numerous studies of alkyl radicals are linked to their role as reactive intermediates in the chemistry of combustion processes [6–9]. In the same way, a strong interest is taken for the chemical reactions of ions in those systems [10,11]. Relative abundance of fragments ions issued from ionization of alkanes with metastable rare gas atoms was investigated by Hiraoka et al. [12]. Photodissociation of heptane and relative ionization efficiencies of main radicals were reported by Brehm [13] and Silva et al. [14].

The removal of volatile organic compounds (VOCs) and hydrocarbons (HCs) in gaseous effluents by means of pulsed electrical discharges is the subject of a growing interest [15–17], but an accurate understanding of the physical and chemical mechanisms involved requires a detailed knowledge of dissociation processes of these molecules by electron impact. In such non-thermal plasmas, the electron energy distribution covers a broad range and data are needed concerning the cross-sections and the type of neutral and/or ionic species produced via the dissociative excitation and ionization collisions on VOCs and HCs. In case of HCs or alcohol molecules, these data should also be useful for a better understanding of the ignition and combustion control by non-thermal plasmas [18,19]. In particular, *n*-heptane has been the subject of recent works about DC-corona discharge, such as the effect of this molecule on ozone production [20], or its removal by the discharge created in dry and in humid air [21,22]. Numerous positive ions coming from the hydrocarbon have been detected in such plasmas [22].

In the present paper, mass spectrometry measurements of the electron impact ionization of *n*-heptane are reported, cross-sections for the formation of fragment ions are measured. Dissociative processes leading to the observed ions are suggested. Such data will be useful for kinetic plasma modelling developed for detailed investigations on HCs conversion processes in plasmas produced by electrical discharges, such as nanoseconds [19] or photo-triggered [23,24] discharges.

2. Experimental and theoretical method

2.1. Experimental

The experimental set-up has been previously described [25–28]. The *n*-heptane (Aldrich, 99%) is introduced at room temperature, through a septum, into a stainless-steel reservoir at 10^{-3} Torr residual pressure. The vapour is then introduced into a gas container at a partial pressure of less than 1 Torr so as to prevent condensation

* Corresponding author. Tel.: +33 169 157 497.
E-mail address: jean-rene.vacher@u-psud.fr (J.R. Vacher).

1387-3806/$ – see front matter © 2010 Elsevier B.V. All rights reserved.
doi:10.1016/j.ijms.2010.07.013

of the alkane. The formation of condensation droplets has to be avoided at cold spots and the stability of the pressure is checked before the addition of argon (Air Liquide, 99.995%) in the gas container. The pressures are measured with a precision of 0.001 Torr. The gas mixture, 3 Torr of equimolecular argon–heptane, is first admitted into a gas-holder at a controlled pressure of 0.5 Torr, and then admitted, through a 50 μm diameter hole, into the analysis chamber. To reduce water impurities, the inlet gas set-up is previously baked so that the remaining pressure is as low as 10^{-7} Torr.

Ions are formed in the ionization chamber (at a constant pressure of 2×10^{-6} Torr) by the impact of a focused electron beam over the energy range 10–86 eV. Based on a comparison with rare gas ionization thresholds, the electron energy is estimated to be measured at ±0.5 eV. The ions are then accelerated, focused and mass analysed in a quadrupole mass spectrometer with a resolution ($M/\Delta M$) better than 400. The various ionic species are detected by means of a channel-electron multiplier followed by a Faraday cup and the collected current then recorded by a computer (which also controls all set-up functions). The ratios of the intensity of alkane ionic fragments to that of Ar^+ ions give the cross-sections for the formation of the fragments relative to that of argon ionization, the partial pressures of *n*-heptane and of argon being known. Several authors have measured the ionization cross-section of argon [29–32] from the threshold of 15.76 eV [33] to more 200 eV. Recent measurement of Rejoub et al. [31] provides very accurate absolute cross-sections. Nevertheless, as we need cross-sections values with a step of 1 or 2 eV under 30 eV, the values of Wetzel et al. [32] are used in the further calculations. By comparison with the values of Rejoub et al., overestimating measured cross-sections of few percents may be possible above 40 eV. For the intensity ratio measurement, the transmission factor caused by mass segregation into the analyser is taken into account [26–28].

It is well known that discrimination effects may result from the extraction process of fragment ions out of the ion source and from the introduction of the ion beam into the mass analyser. This discrimination is due to the formation of fragment ions from a molecule with a kinetic energy of several electron volts and with a velocity component normal to the axis of the system. This discrimination reduces the number of detected ions of a given mass [34] and thus reduces the cross-section for the formation of this ion. Detailed analyses of the experimental uncertainties in measurements of absolute partial cross-section have been given by Straub et al. [30] and Jiao et al. [35]. It is important to verify the complete collection of the energetic fragment ions in order to obtain conclusive measurements [36]. In order to test the validity of our measurements, we measured ionization cross-section of a heavy molecule. We used *n*-octane for which cross-sections for the formation of ions were measured by Jiao et al. [37]. We checked for masses 43, 41, 85, 57, 29, 71, 56 and 114 at 20, 50 and 70 eV. For these values, our results were consistent with those of Jiao et al. within 20%. These results seem to indicate that no severe discrimination occurs in our apparatus for these masses and these energies.

2.2. Theoretical

The geometrical optimisations and the total electronic energies for the studied molecules, radicals and ions of which data are not given in the literature, were performed with the 6−311G(d,p) basic set using the B3LYP theoretical method. This level basic set allows to optimise the determination of structures and to compare the enthalpies of formation of the species. The ionization energies were computed as being the difference between the enthalpies of the fully optimised neutral molecules or radicals and that of the corresponding radical cations. The use of larger basic sets does not modify significantly the relative energies. All the optimised geometries corresponding to a minimum point have real frequencies. Thermodynamic gas-phase data were computed at 298.15 K and 1 atmosphere using the internal thermal energy and the absolute entropy of each species. Ab initio calculations were carried out using the Gaussian 03 series of programs [38].

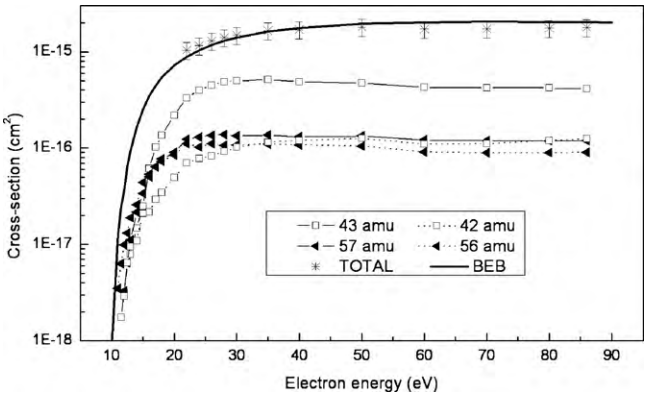

Fig. 1. Cross-sections for the formation of four major cations issued from *n*-heptane. Total ionization cross-section measured for the formation of ions issued from *n*-heptane above 20 eV and calculated with BEB theory from 10 eV to 90 eV.

The cross-section for ejecting an electron from an orbital by electron impact can be calculated using the Binary–Encounter–Bethe (BEB) model developed by Kim et al. for atoms [39] and molecules [40]. This cross-section is given by:

$$\sigma_{\mathrm{BEB}}(T) = \frac{S}{t+u+1}\left[\frac{Q\ln t}{2}\left(1-\frac{1}{t^2}\right)+(2-Q)\left(1-\frac{1}{t}-\frac{\ln t}{t+1}\right)\right]$$

where $S = 4\pi a_o{}^2 N(R/B)^2$ with $a_o = 0529$ Å, $R = 13.61$ eV, N = electron occupation number, B = orbital binding energy, $t = T/B$ with the incident electron kinetic energy T, $u = U/B$ with the orbital kinetic energy U and Q is an integral on the continuum dipole oscillator strength which to a good approximation is routinely set equal to 1 [41]. The total single ionization cross-section is given by the sum over all the occupied molecular orbitals:

$$\sigma(T) = \sum \sigma_{\mathrm{BEB}}(T)$$

The values of each orbital binding energy and orbital kinetic energy of *n*-heptane in the ground state were obtained using ab initio calculations at the classical RHF/STO-3G level of theory which gives reliable values of orbital binding energies. Twenty two of these orbitals contribute to the BEB cross-section below 100 eV. To ensure that cross-section starts at the ionization threshold, the calculated binding energy of the highest occupied molecular orbital (HOMO) is replaced by the experimental value of the ionization energy. The results of theoretical determinations of electron impact ionization cross-sections depend on the ab initio level of theory used [42,43]. With no empirical corrections to the binding energies, the BEB method gives cross-sections slightly lower than those measured [44]. Empirically adjusted orbital energies can reconcile the difference between computed and measured cross-sections but such corrections were not taken into account in our study.

3. Results and discussion

About forty different masses are observed but only fifteen of them have been selected: those whose ionization cross-section is greater than 1×10^{-18} cm^2 at 86 eV (Table 1). The cross-sections for the formations of these $C_nH_m{}^+$ ions which contribute to 95% of the total ionization of *n*-heptane are shown between 10 eV and 86 eV in Figs. 1–3. Fig. 4 shows the cross-sections for the formations of ions from 10 eV to 20 eV in order to detail the results in the vicinity of the threshold. We estimate, according to Section 2, that the uncer-

Table 1
Cross-sections σ ($\times 10^{-16}$ cm^2) for the formation of the main ions from *n*-heptane at 86 eV (maximum voltage used), 30 eV and 12 eV (near the threshold).

Mass (amu)	86 eV		30 eV		12 eV	
	σ	σ Relativity (%)	σ	σ Relativity (%)	σ	σ Relativity (%)
43	4.1	23	5.0	34	0.032	6.4
41	3.0	17	2.3	15	–	–
29	1.4	7.9	0.78	5.2	–	–
27	1.3	7.3	0.17	1.1	–	–
39	1.3	7.3	0.087	0.58	–	–
42	1.2	6.7	1.0	6.7	0.029	5.8
57	1.2	6.7	1.3	8.7	0.033	6.6
71	1.1	6.2	1.1	7.4	0.11	22
56	0.90	5.0	1.1	7.4	0.10	20
100	0.80	4.5	0.90	6.0	0.13	26
70	0.62	3.5	0.67	4.5	0.066	13
55	0.41	2.3	0.39	2.6	–	–
28	0.39	2.2	0.10	0.67	–	–
85	0.068	0.38	0.061	0.41	–	–
15	0.037	0.21	–	–	–	–

Ions are listed in order of decreasing cross-section for 86 eV.

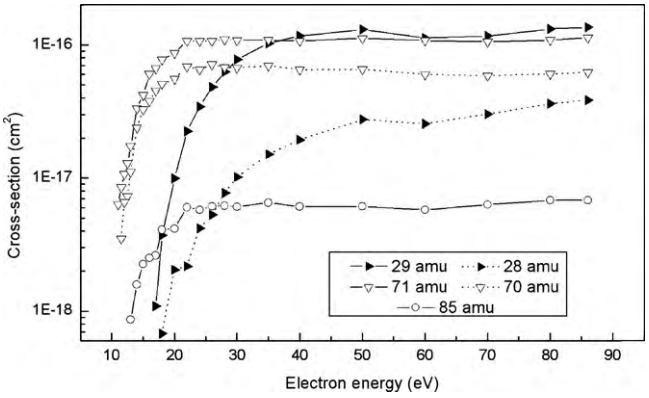

Fig. 2. Cross-sections for the formation of five cations issued from *n*-heptane.

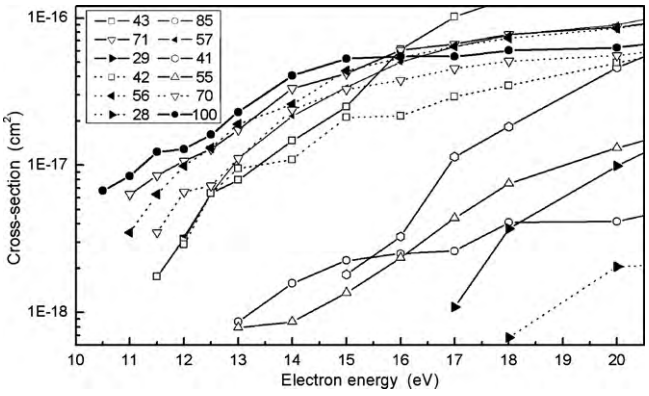

Fig. 4. Cross-sections for the formation of 12 ions issued from *n*-heptane between 10 eV and 20 eV. Masses are given in amu.

tainty in the given values is 20%. The total ionization cross-section in Fig. 1 is the sum of all the cross-sections listed in Table 1. Details of the cross-sections plotted in Fig. 1 are given in Table 2. The measured total cross-section for ions formation from *n*-heptane rises up to 30 eV and reaching a maximum value of 1.5×10^{-16} cm^2 at around 50 eV before a slight decrease until 86 eV, the maximum usable voltage.

The measured total cross-section of *n*-heptane in Fig. 1 agrees well with the cross-section given by the theoretical model between 20 eV and 86 eV. The differences between the experimental data and the data given by the model are compatible with the exper-

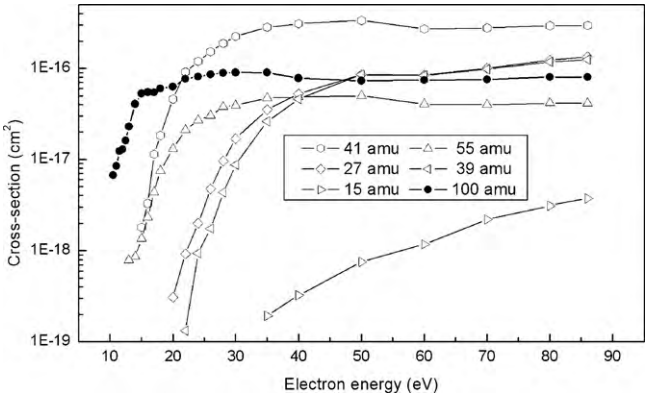

Fig. 3. Cross-sections for the formation of the molecular ion (black circles). Cross-sections of five cations issued from *n*-heptane via ionization of C_4H_9.

Table 2
Values of the cross-sections ($\times 10^{-16}$ cm^2) for the formation of the four ions shown in Fig. 1. The total ionization cross-section measured and given by the BEB model are also included.

V (eV)	$C_3H_6^+$	$C_3H_7^+$	$C_4H_8^+$	$C_4H_9^+$	Total	BEB
90						20.3
86	1.25	4.14	0.90	1.20	17.9	20.4
80	1.20	4.21	0.90	1.19	17.6	20.5
70	1.11	4.23	0.89	1.20	17.3	20.6
60	1.10	4.29	0.91	1.22	17.2	20.3
50	1.26	4.74	1.05	1.34	18.1	19.5
40	1.20	4.92	1.08	1.31	17.0	17.7
35	1.15	5.16	1.10	1.37	16.6	16.2
30	1.02	4.99	1.08	1.34	14.9	14.0
28	0.92	4.89	1.07	1.39	14.1	13.0
26	0.83	4.52	1.11	1.36	13.0	11.8
24	0.78	3.99	1.03	1.30	11.6	10.4
22	0.70	3.34	1.11	1.24	10.4	8.90
20	0.49	2.19	0.85	0.90		7.24
18	0.35	1.36	0.73	0.77		5.43
17	0.29	1.02	0.64	0.64		4.45
16	0.22	0.61	0.54	0.50		3.48
15	0.21	0.25	0.44	0.34		2.52
14	0.11	0.15	0.26	0.22		1.68
13	0.095	0.079	0.19	0.11		0.93
12.5	0.064	0.064	0.13	0.064		0.64
12	0.029	0.032	0.099	0.033		0.36
11.5		0.017	0.063			0.25
11			0.035			0.13
10.5						0.067
10						0.008

imental uncertainties mentioned previously as shown with the error bars. Between 10 eV, just above the ionization threshold of *n*-heptane (9.93 eV [33]) and 20 eV, the cross-section of each of observed ions is calculated in order to normalize the sum to the value given by the BEB model. Between 20 eV and 25 eV, our results are slightly higher than those given by the theoretical model. As the BEB model underestimates our experimental results, the cross-sections of these ions may be underestimated in the range 10–20 eV, but this does not change the considerations as to the formation of each of these ions. No signal was measured below 10.5 eV.

The formation of an appreciable number of ions from *n*-C_7H_{16} results from primary processes: the kinetic energy resulting from the electron collision is converted into internal energy leading to the dissociation of the ion into a smaller one and a neutral fragment. The fact that the molecular ion is observed over the whole range of ionization energy (Fig. 3) suggests that the formation of an appreciable number of ions results directly from the fragmentation of the molecular ion via a simple bond splitting process, leading to C_nH_{2n+1} cation, or via a bond splitting followed by H-atom transfer between the two fragments, leading to C_nH_{2n} cation.

In the following, the formation of some ions considered in Table 1 will be explained as the result either of a simple bond splitting of the molecular ion, or of bond splitting followed by rearrangements. If different isomers describe cations, we shall consider the first one resulting of a bond split without rearrangement and with a linear structure and the second one having the minimum enthalpy of formation. It will be tried to understand the formation of the other ions issued from *n*-heptane. The results will be compared with results of other alkanes given in the literature.

3.1. The molecular ion

Fig. 3 shows that the cross-section for the formation of the ion of mass $M = 100$ amu is close to 8×10^{-17} cm^2 between 86 eV and 30 eV, decreases slowly to 15 eV and then clearly to 10.5 eV, near the ionization threshold. The molecular ion contributes to about 5% of the total cross-section at the maximum voltage; it becomes the most abundant below 15.5 eV (Fig. 4) and represents 100% of the total cross-section near the threshold. It should be pointed out that the molecular ion is observed in *n*-heptane whereas it is missing with isomeric molecules containing two methyl groups on the same carbon (2,2-dimethylpentane, 2,2,3-trimethylbutane, . . .) [33]. The same trends are observed with other alkanes such as *n*-octane and 2,2,4-trimethylpentane [37,25].

3.2. Ions issued from a simple bond split

3.2.1. $C_3H_7^+$

The ion of 43 amu is the most abundant between 86 eV and 16 eV (Fig. 1). The cross-section is close to 5×10^{-16} cm^2 and contributes to about 30% of the total cross-section between 86 eV and 26 eV. At lower energies, its contribution decreases quickly. This ion is still detected at 11.5 eV, just above the ionization threshold, contributing 5% of the total cross-section. Reaction (1) in Table 3 results from a simple C–C bond split between the C3 and the C4 in the molecular ion and reaction (2) results from the same bond split but with a H-atom migration. The two produced ionic species may be described as being 1-propyl cation with the first reaction and 2-propyl (isopropyl) cation with the second one. Table 3 shows that the dissociations of the molecular ions are endothermic. Values of ΔE give the threshold energy to obtain ions and C_4H_9 (butyl radical) from neutral *n*-heptane. The minimum voltage for which the ion of 43 amu is observed is 11.5 ± 0.5 eV (see Fig. 4), this value is very close to the ΔE of reactions (1) and (2) and it is not easy to choose the true ionic species of 43 amu. In the column "Rule" of Tables 3 and 4, the word yes or no indicates that the Stevenson's rule, which stipulates that the fragment of lowest ionization energy retains the charge and becomes the ionic fragment [45], is respected or not in the dissociation process considered. This rule being not respected with reaction (1), we can conclude that the ion of 43 amu is the isopropyl cation issued from reaction (2), which is the less endothermic of these two reactions. This conclusion is consistent with theoretical study of Takeuchi et al. [46] on the fragmentation of *n*-butane cation; the isopropyl cation has been calculated to be the most stable $C_3H_7^+$ species.

3.2.2. $C_2H_5^+$

The cross-section for the formation of the ethyl cation (Fig. 2) is about 1.4×10^{-16} cm^2 between 86 eV and 40 eV and then decreases slowly as the energy drops to 17 eV. The difference between ionization energies of the two species issued from reaction (3) is low (0.2 eV), C_5H_{11} having the smaller I.E than C_2H_5. Ethyl ion is not observed at low electron energy ($\leq$16 eV) when $C_5H_{11}^+$ is present near the threshold. Fig. 2 shows that the $C_2H_5^+$ cross-section rises more slowly than the $C_5H_{11}^+$ cross-section but the two values become similar above 40 eV. Although the Stevenson's rule is not strictly respected, a C–C bond split between the C2 and the C3 atoms of *n*-$C_7H_{16}^+$ may lead to $C_2H_5^+$ as well as that $C_5H_{11}^+$ above 17 eV.

3.2.3. $C_4H_9^+$

The cross-section for the formation of this ion of 57 amu is close to 1.2×10^{-16} cm^2 between 86 eV and 22 eV and then decreases quickly, contributing 6.6% to the total cross-section at 12 eV, the minimum voltage for which this ion is observed. The structure of butyl cations issued from ionization of some alkanes have been investigated by Shold and Ausloos [47]. The tert-butyl (2-methyl-2-propyl) ion is thermodynamically the most stable whereas the 1-butyl, 2-butyl and the isobutyl cations are slightly less stable [48,49]. Reaction (6) in Table 3 results from a simple C–C bond split between the C3 and the C4 in the molecular ion and reaction (7) results from the same bond split but with a methyl group migration. ΔE of reactions (6) and (7) are calculated for the production of 1-butyl and tert-butyl cations with 1-propyl radical, respectively. As these values are below 12 eV, both ionic species are able to be produced. Yet, we can note that reaction (6) is largely endothermic whereas reaction (7) is slightly endothermic. So, the formation of the tert-butyl cation occurs preferentially, via a rearrangement before or during the bond cleavage in the molecular ion.

3.2.4. $C_5H_{11}^+$

The ion of 71 amu is one of the more abundant near the threshold, contributing to 35% of the total cross-section at 11 eV. The cross-section for the formation of this ion is constant and close to 1.1×10^{-16} cm^2 between 86 eV and 22 eV. From the five possible isomeric structures of pentyl cations, the tert-pentyl (2-methyl-2-butyl) ion is thermodynamically the most stable [50]. Reaction (8) in Table 3 results from a simple C–C bond split between the C2 and the C3 in the molecular ion and reaction (9) results from the same bond split but with a methyl group migration. ΔE values are calculated for the formation of 1-pentyl and tert-pentyl. Table 3 shows that ΔE value for reaction (8) is above 11 eV, the minimum energy for which the ion is observed, while for reaction (9) it is below. Thus, we can conclude that the ion of 71 amu is the tert-pentyl ion issued from reaction (9) which is the least endothermic of these two reactions.

3.2.5. $C_6H_{13}^+$

This is one of the two minor ions observed. The cross-section (Fig. 2) is close to 6.5×10^{-18} cm^2 and contributes to only 0.4% of the total cross-section between 86 eV and 22 eV. At lower energies, its contribution decreases quickly but the ion is still detected up

Table 3
Possible dissociation reactions of molecular cation, leading to the detected ions. These reactions result either from a simple C–C bond split process (odd masses) or a bond split with a H-atom rearrangement (even masses).

Mass of the ion	Reaction	ΔE (eV)	Rule	$\Delta_r H^\circ$ (kJ mol^{-1})
43	(1) $C_7H_{16}^+ \rightarrow C_3H_7^+ + C_4H_9$	11.75	No	176
43	(2) $C_7H_{16}^+ \rightarrow$ i-$C_3H_7^+ + C_4H_9$	10.92	Yes	96
29	(3) $C_7H_{16}^+ \rightarrow C_2H_5^+ + C_5H_{11}$	11.79	Yes?	179
42	(4) $C_7H_{16}^+ \rightarrow C_3H_6^+ + C_4H_{10}$	10.58	Yes	63
42	(5) $C_7H_{16}^+ \rightarrow$ c-$C_3H_6^+ + C_4H_{10}$	11.06	Yes	109
57	(6) $C_7H_{16}^+ \rightarrow C_4H_9^+ + C_3H_7$	11.68	Yes	169
57	(7) $C_7H_{16}^+ \rightarrow$ t-$C_4H_9^+ + C_3H_7$	10.18	Yes	24
71	(8) $C_7H_{16}^+ \rightarrow C_5H_{11}^+ + C_2H_5$	11.51	Yes	152
71	(9) $C_7H_{16}^+ \rightarrow$ t-$C_5H_{11}^+ + C_2H_5$	10.13	Yes	19
56	(10) $C_7H_{16}^+ \rightarrow$ 1-$C_4H_8^+ + C_3H_8$	10.41	Yes	46
56	(11) $C_7H_{16}^+ \rightarrow$ 2-$C_4H_8^+ + C_3H_8$	9.93	Yes	−8
70	(12) $C_7H_{16}^+ \rightarrow C_5H_{10}^+ + C_2H_6$	10.33	Yes	39
70	(13) $C_7H_{16}^+ \rightarrow$ i-$C_5H_{10}^+ + C_2H_6$	9.93	Yes	−57
28	(14) $C_7H_{16}^+ \rightarrow C_2H_4^+ + C_5H_{12}$	11.48	Yes?	149
85	(15) $C_7H_{16}^+ \rightarrow C_6H_{13}^+ + CH_3$	11.67	Yes	168
85	(16) $C_7H_{16}^+ \rightarrow$ t-$C_6H_{13}^+ + CH_3$	10.19	Yes	25
15	(17) $C_7H_{16}^+ \rightarrow CH_3^+ + C_6H_{13}$	13.59	No	353

Neutral species are considered having linear structures.

to 13 eV. This ion of 85 amu is issued from a simple C–C bond split between the C1 and the C2 in the molecular ion, in resulting the lost of a methyl group. It should be pointed out that fragments ions M-15 are completely missing in *n*-C_8H_{18} [37] which is a characteristic cracking pattern when linear alkane molecule become large [51]. Calculated enthalpy of formation of 1-hexyl is 28 kJ mol^{-1}. With −8 kJ mol^{-1}, the tert-hexyl (2-methyl 2-pentyl) ion is found to be the most stable of isomers of hexyl ions [50]. Reaction (15) in Table 3 results from a simple C–C bond split and reaction (16) results from the same bond split but with a methyl group migration. ΔE values are calculated for the formation of 1-hexyl and tert-hexyl ions from *n*-heptane. Table 3 shows that ΔE value for these two reactions are below 13 eV. However, we observe that reaction (16) is much less endothermic than reaction (15). So, the formation of the tert-hexyl cation occurs preferentially, via a rearrangement before or during the bond cleavage in the molecular ion.

3.2.6. CH_3^+

The methyl cation is the minor ion observed. Fig. 3 shows that its cross-section decreases steadily from 86 eV to 35 eV, the minimum voltage for which this ion is observed. As the Stevenson's rule is not respected in the reaction (17), the methyl ion cannot be issued from a simple C–C bond cleavage in the molecular ion. Another path leading to the methyl must be found.

3.3. Ions issued from a bond split with H-atom rearrangement

Cross-sections for the formation of $C_nH_{2n}^+$ cations for $2 \leq n \leq 5$ are drown with dot lines in Figs. 1 and 2 together with cross-sections of correspondent $C_nH_{2n+1}^+$ cations drown with straight lines. It can be seen that, for each of theses four series, cross-sections of $C_nH_{2n}^+$ rise slower and are lower (except for $n = 4$ under 17 eV as shown in Fig. 4).

3.3.1. $C_3H_6^+$

The cross-section for the formation of this ion of 42 amu is close to 1.2×10^{-16} cm^2 between 86 eV and 35 eV (Fig. 1) and then decreases to 12 eV, the minimum voltage for which this ion is observed. Two produced ionic species are described as being propene cation with reaction (4) and cyclopropane cation with reaction (5). These two reactions result as for $C_3H_7^+$, from a C–C bond split between C3 and C4 but in this case via a H-atom rearrangement between the two fragments, before or during the bond cleavage. As it as been observed with *n*-octane [37], the bond cleavage with rearrangement has a relatively small activation energy as compared to the simple bond cleavage. We note that reaction (4) has a small ΔE and is less endothermic than reaction (5) and reaction (2) leading $C_3H_7^+$. So, the formation of the propene cation can occur preferentially near the threshold, via a H-atom rearrangement.

3.3.2. $C_4H_8^+$

The ion of 56 amu is abundant near the threshold, contributing to 19% of the total cross-section at 11 eV. The cross-section for the formation of this ion is similar of the one of $C_5H_{11}^+$ and close to 1.1×10^{-16} cm^2 between 86 eV and 22 eV (Fig. 1). From six possible isomers, the 2-butene(E) cation is thermodynamically the most stable [33]. The two reactions (10) and (11) result from a C–C bond split with a H-atom rearrangement as for $C_3H_6^+$, yielding 1-butene and 2-butene cations. As reaction (11) is exothermic, ΔE of the reaction is the ionization energy of *n*-heptane as thus 2-butene cation may be present since the threshold but 1-butene cation may also be present just above as shown ΔE of reaction (10).

3.3.3. $C_5H_{10}^+$

The cross-section for the formation of the ion of 70 amu is close to 6.5×10^{-17} cm^2 between 86 eV and 22 eV (Fig. 2) and then decreases quickly, still contributing 18% to the total cross-section at

Table 4
Possible dissociation reactions leading to the detected ions from collision of butyl radical with energetic electrons.

Mass of the ion	Reaction	Rule	$\Delta_r H^\circ$ (kJ mol^{-1})	$\Delta_r H^\circ$ (eV)	Observed (eV)
41	(18) $C_4H_9 \rightarrow C_3H_5^+ + CH_3 + H$	yes	1259	13.05	15
27	(19) $C_4H_9 \rightarrow C_2H_3^+ + 2CH_3$	Yes	1321	13.70	20
39	(20) $C_4H_9 \rightarrow$ c-$C_3H_3^+ + CH_3 + 3H$	Yes	1910	19.80	22
55	(21) $C_4H_9 \rightarrow C_4H_7^+ + H_2$	Yes	938	10.92[a]	13
15	(22) $C_4H_9 \rightarrow CH_3^+ +$ c-C_3H_6	Yes	1069	11.08	30

Species are considered having linear structures except cyclopropenyl and cyclopropane.
[a] From reaction (2) in Table 3.

11.5 eV, the minimum voltage for which this ion is observed. From the possible isomeric structures of pentene cations, isopentene (2-methyl-2-butene) ion is found thermodynamically the most stable [33]. Reactions (12) and (13) yield, via H-atom rearrangement, 1-pentene and isopentene. As reaction (13) is exothermic, ΔE of the reaction is the ionization energy of *n*-heptane. As for the formation of $C_4H_8^+$, isopentene cation may be present since the threshold but 1-pentene cation may also be present above as shown ΔE of reaction (12).

3.3.4. $C_2H_4^+$

The cross-section of the ethene cation is close to 3×10^{-17} cm^2 between 86 eV and 50 eV and then decreases steadily to 18 eV, the minimum voltage for which this ion is observed. The difference between ionization energies of the two species issued from reaction (14) is 0.2 eV, C_5H_{12} having the smaller I.E. Ethene ion is not observed below 18 eV and $C_5H_{10}^+$ is detected near the threshold. The $C_2H_4^+$ cross-section rises slowly, as for the one of ethyl cation (Fig. 2). It is thus possible that a C–C bond split between the C2 and the C3 atoms of *n*-$C_7H_{16}^+$ may lead to $C_2H_4^+$ and pentane molecule.

3.4. Ions issued from the fragmentation of C_4H_9

The major neutral fragment is issued from reaction (2) with the formation of the majority ion $C_3H_7^+$. Collision of neutral C_4H_9 with energetic electrons can lead, via C–C and C–H bond splits to five of the observed ions. The possible channels leading to the detected ions are given for a minimum atom rearrangement and by order of decreasing intensities in Table 4. The enthalpy changes show that the formations of theses ionic species are largely endothermic.

$C_3H_5^+$, the most abundant of these five ions (Fig. 3), may be identified as allyl cation, thermodynamically more stable than cyclopropyl cation [33]. The measured cross-section, which represents over 15% of the total ionization cross-section of *n*-heptane, is slightly constant from 86 eV to 35 eV and decreases to 15 eV, the minimum energy to observe this ion. The cross-section for the formation of $C_4H_7^+$, possible 1-butene-1-yl without rearrangement, is also constant from 86 eV to 35 eV, representing 2.5% of the total cross-section and decreases to the minimum energy of 13 eV. Calculated enthalpy of formation and ionization energy of C_4H_7 are 227 kJ mol^{-1} and 8.04 eV. Enthalpy change for reaction (21) is found less than ΔE of reaction (2), thus the true energy to form $C_4H_7^+$ from *n*-heptane is 10.92 eV. The cross-sections for the formation of vinyl cation decreases slightly from 86 eV to 50 eV and then rapidly to 20 eV. The same trend is observed with ion of 39 amu identified as being the more thermodynamically stable propargyl cation than the cyclopropenyl cation. It should be noted that enthalpy changes for these fragmentation processes are lower than the minimum electron energies required to observe these ions with our experimental device (see right column in Table 4).

Methyl ion may be issued from C_4H_9 by reaction (22); C_3H_6 being propene or cyclopropane. As the Stevenson's rule is not respected with this first molecule, we suppose that the formation of CH_3^+ is associated with the one of c-C_3H_6. The fact that the methyl cation is not detected at low energy (<30 eV) is due to the detection limit of our apparatus. Electron impact ionization of methyl radicals issued from reaction (15) or (16) can also yield methyl cations but since $C_6H_{13}^+$ is a minority ion, the formation of methyl cation via this process is very weak.

4. Conclusion

Electron impact ionization of *n*-heptane produces molecular and fragment ions with a total ionization cross-section of 1.5×10^{-16} cm^2 towards 50 eV. Cross-sections for the formation of the major species are measured between 10 eV and 86 eV. The present results are in good agreement with the total ionization cross-sections measured and obtained from the BEB theory. The molecular ion is the most abundant below 16 eV and $C_3H_7^+$, identified as isopropyl cation, becomes the most abundant cation above 16 eV. Five ions $C_nH_{2n+1}^+$ ($2 \le n \le 6$) result from a simple C–C bond split in the molecular ion and four ions $C_nH_{2n}^+$ ($2 \le n \le 5$) result from a C–C bond split with H-atom rearrangement. For the same n, cross-sections for the formation of the ionic species of the second series rise slower and are lower above 17 eV. Five other ions, $C_nH_{2n-1}^+$ ($2 \le n \le 4$), $C_3H_3^+$ and CH_3^+ may result from the ionization of C_4H_9, the major alkyl issued from the fragmentation of the molecular ion. Ionization energies as well as enthalpies of dissociation reactions allow the identification of the principal ionic species.

References

[1] N. Blin-Simiand, R. Rigny, V. Viossat, S. Circan, K. Sahetchian, Combust. Sci. Technol. 88 (1993) 329–348.
[2] A.T. Ingemarsson, J.R. Pedersen, J.O. Olsson, J. Phys. Chem. A 103 (1999) 8222–8230.
[3] H.J. Curran, P. Gafferi, W.J. Pitz, C.K. Westbrook, Combust. Flame 114 (1998) 149–177.
[4] J Song, C. Yao, S. Liu, Z. Tian, J. Wang, Fuel 88 (2009) 2297–2302.
[5] R. Minetti, M. Carlier, M. Ribaucour, E. Therssen, L.R. Sochet, Combust. Flame 102 (1995) 298–309.
[6] C.K. Westbrook, Proc. Combust. Inst. 28 (2) (2000) 1563–1577.
[7] N. Yamauchi, A. Miyoshi, K. Kosaka, M. Koshi, H. Matsui, J. Phys. Chem. A 103 (1999) 2723–2733.
[8] N. Blin-Simiand, F. Jorand, K. Sahetchian, M. Brun, L. Kerhoas, C. Malosse, J. Einhorn, Combust. Flame 126 (1–2) (2001) 1524–1532.
[9] J Warnatz, Pure Appl. Chem. 72 (11) (2000) 2101–2110.
[10] A.B. Fialkov, Prog. Energy Combust. Sci. 23 (1997) 399–528.
[11] J. Prager, U. Riedel, J. Warnatz, in: Proc. of the 31st Symp. on Combustion, 2007, pp. 1129–1137.
[12] K. Hiraoka, H. Furuya, S. Kambara, S. Suzuki, H. Hashimoto, A. Takamizawa, Rapid. Commun. Mass Spectrom. 20 (2006) 3213–3222.
[13] B. Brehm, Z. Naturforschg 21a (1966) 196–209.
[14] R. Silva, W.K. Gichuhi, M.B. Doyle, A.H. Winney, A.G. Suits, Phys. Chem. Chem. Phys. 11 (2009) 4777–4781.
[15] K. Vercammen, A. Berezin, J. Adv. Oxid. Technol. 2 (1997) 312–318.
[16] H.-H. Kim, Plasma Process. Polym. 1 (2004) 91–110.
[17] J. Van Durme, J. Dewulf, C. Leys, H. Van Langenhove, Appl. Catal. B: Environ. 78 (2008) 324–333.
[18] S. Starikovskaia, J. Phys. D: Appl. Phys. 39 (2006) R265–R299.
[19] I. Kosarev, N. Aleksandrov, S. Kindysheva, S. Starikovskaia, A. Starikovskii, Combust. Flame 156 (2009) 221–233.
[20] S. Pekarek, J. Phys. D: Appl. Phys. 41 (2008) 025204 (6pp).
[21] E. Marotta, A. Callea, X. Ren, M. Rea, C. Paradisi, Int. J. Plasmas Environ. Sci. Technol. 1 (2007) 39–45.
[22] E. Marotta, A. Callea, X. Ren, M. Rea, C. Paradisi, Plasma Process. Polym. 5 (2008) 146–154.
[23] S. Pasquiers, C. Postel, L. Magne, V. Puech, G. Lombardi, J. Adv. Oxid. Technol. 7 (2004) 108–115.
[24] L. Magne, S. Pasquiers, K. Gadonna, P. Jeanney, N. Blin-Simiand, F. Jorand, C. Postel, J. Phys. D: Appl. Phys. 42 (165203) (2009) (17pp).
[25] K. Bouamra, J.R. Vacher, F. Jorand, N. Simiand, S. Pasquiers, Chem. Phys. Lett. 373 (2003) 237–244.
[26] J.R. Vacher, F. Jorand, N. Blin-Simiand, S. Pasquiers, Chem. Phys. Lett. 434 (2007) 188–193.
[27] J.R. Vacher, F. Jorand, N. Blin-Simiand, S. Pasquiers, Int. J. Mass Spectrom. 273 (2008) 117–125.
[28] J.R. Vacher, F. Jorand, N. Blin-Simiand, S. Pasquiers, Chem. Phys. Lett. 476 (2009) 178–181.
[29] E. Krishnakumar, S.K. Srivastava, J. Phys. B 21 (1988) 1055–1082.
[30] H.C. Straub, P. Renault, B.G. Lindsay, K.A. Smith, R.F. Stebbings, Phys. Rev. A 52 (1995) 1115–1124.
[31] R. Rejoub, B.G. Lindsay, R.F. Stebbings, Phys. Rev. A 65 (2002) 42713 (8pp).
[32] R.C. Wetzel, F.A. Baiocchi, T.R. Hayes, R.S. Freund, Phys. Rev. A 35 (1987) 559–577.
[33] NIST database, available at: http://webbook.nist.gov/chemistry/. Original references for data can be obtained from this database.
[34] C.E. Berry, Phys. Rev 78 (1950) 597–605.
[35] C.Q. Jiao, R. Nagpal, P.D. Haaland, Chem. Phys. Lett. 269 (1997) 117–121.
[36] C. Tian, C.R. Vidal, J. Phys. B 31 (1998) 5369–5381.
[37] C.Q. Jiao, C.A. Dejoseph Jr., A. Garscadden, J. Chem. Phys. 114 (2001) 2166–2172.
[38] M.J. Frisch, G.W. Trucks, H.B. Schlegel, G.E. Scuseria, M.A. Robb, J.R. Cheeseman, J.A. Montgomery, Jr., T.Vreven, K.N. Kudin, J.C. Burant, J.M. Millam, S.S. Iyengar, J. Tomasi, V. Barone, B. Mennucci, M. Cossi, G. Scalmani, N. Rega, G.A. Petersson, H. Nakatsuji, M. Hada, M. Ehara, K. Toyota, R. Fukuda, J. Hasegawa, M. Ishida, T. Nakajima, Y. Honda, O. Kitao, H. Nakai, M. Klene, X. Li, J.E. Knox, H.P. Hratchian, J.B. Cross, C. Adamo, J. Jaramillo, R. Gomperts, R.E. Stratmann, O. Yazyev, A.J.

Austin, R. Cammi, C. Pomelli, J.W. Ochterski, P.Y. Ayala, K. Morokuma, G.A. Voth, P. Salvador, J.J. Dannenberg, V.G. Zakrzewski, S. Dapprich, A.D. Daniels, M.C. Strain, O. Farkas, D.K. Malick, A.D. Rabuck, K. Raghavachari, J.B. Foresman, J.V. Ortiz, Q. Cui, A.G. Baboul, S. Clifford, J. Cioslowski, B.B. Stefanov, G. Liu, A. Liashenko, P. Piskorz, I. Komaromi, R.L. Martin, D.J. Fox, T. Keith, M.A. Al-Laham, C.Y. Peng, A. Nanayakkara, M. Challacombe, P.M.W. Gill, B. Johnson, W. Chen, M. W. Wong, C. Gonzalez, J.A. Pople, Gaussian 03, Revision C.02, Gaussian, Inc., Wallingford CT, 2004.
[39] Y.K. Kim, M.E. Rudd, Phys. Rev. A 50 (1994) 3954–3966.
[40] W. Hwang, Y.K. Kim, M.E. Rudd, J. Chem. Phys. 104 (1996) 2956–2966.
[41] M.A. Ali, Y.K. Kim, W. Hwang, N.M. Weinberger, M.E. Rudd, J. Chem. Phys. 106 (1997) 9602–9608.
[42] P.D. Haaland, C.Q. Jiao, A. Garscadden, Chem. Phys. Lett. 340 (2001) 479–483.
[43] H. Deutsch, K. Becker, S. Matt, T.D. Märk, Int. J. Mass Spectrom. 197 (2000) 37–69.
[44] C.Q. Jiao, A. Garscadden, P.D. Haaland, Chem. Phys. Lett. 310 (1999) 52–56.
[45] F.W. McLafferty, F. Tureček, Interpretation of Mass Spectra, 4th ed., University science Books, Sausalito, CA, 1993.
[46] T. Takeuchi, M. Yamamoto, K. Nishimoto, H. Tanaka, K. Hirota, Int. J. Mass Spectrom. 52 (1983) 139–148.
[47] D.M. Shold, P. Ausloss, J. Am. Chem. Soc. 100 (1978) 7915–7919.
[48] M. Boronat, P. Viruela, A. Corma, J. Phys. Chem. 100 (1996) 633–637.
[49] P. Campomanes, D. Suárez, T.L. Sordo, J. Phys. Chem. 103 (1999) 5996–6002.
[50] F.P. Lossing, A. MacColl, Can. J. Chem. 54 (1976) 990–992.
[51] A. MacColl, Org. Mass Spectrom. 17 (1982) 1–9.